

**REPORT DOCUMENTATION PAGE**

*Form Approved  
OMB No. 0704-0188*

The public reporting burden for this collection of information is estimated to average 1 hour per response, including the time for reviewing instructions, searching existing data sources, gathering and maintaining the data needed, and completing and reviewing the collection of information. Send comments regarding this burden estimate or any other aspect of this collection of information, including suggestions for reducing the burden, to Department of Defense, Washington Headquarters Services, Directorate for Information Operations and Reports (0704-0188), 1215 Jefferson Davis Highway, Suite 1204, Arlington, VA 22202-4302. Respondents should be aware that notwithstanding any other provision of law, no person shall be subject to any penalty for failing to comply with a collection of information if it does not display a currently valid OMB control number.  
**PLEASE DO NOT RETURN YOUR FORM TO THE ABOVE ADDRESS.**

<b>1. REPORT DATE (DD-MM-YYYY)</b> 06/30/2016		<b>2. REPORT TYPE</b> Technical Report (Quarterly)		<b>3. DATES COVERED (From - To)</b> 04/01/2016 - 06/30/2016	
<b>4. TITLE AND SUBTITLE</b> A Hybrid Approach to Composite Damage and Failure Analysis Combining Synergistic Damage Mechanics and Peridynamics				<b>5a. CONTRACT NUMBER</b>	
				<b>5b. GRANT NUMBER</b> N00014-16-1-2173	
				<b>5c. PROGRAM ELEMENT NUMBER</b>	
<b>6. AUTHOR(S)</b> Dr. Ramesh Talreja				<b>5d. PROJECT NUMBER</b>	
				<b>5e. TASK NUMBER</b>	
				<b>5f. WORK UNIT NUMBER</b>	
<b>7. PERFORMING ORGANIZATION NAME(S) AND ADDRESS(ES)</b> Texas A&M Engineering Experiment Station (TEES) 1470 William D. Fitch Parkway College Station, TX 77845				<b>8. PERFORMING ORGANIZATION REPORT NUMBER</b> M1601473 / 505170-00001/2	
<b>9. SPONSORING/MONITORING AGENCY NAME(S) AND ADDRESS(ES)</b> Office of Naval Research 875 N. Randolph Street Suite 1425 Arlington, VA 22203-1995				<b>10. SPONSOR/MONITOR'S ACRONYM(S)</b> ONR	
				<b>11. SPONSOR/MONITOR'S REPORT NUMBER(S)</b>	
<b>12. DISTRIBUTION/AVAILABILITY STATEMENT</b> unlimited					
<b>13. SUPPLEMENTARY NOTES</b>					
<b>14. ABSTRACT</b> The work performed in the reporting period has been focused on continuation of Task 1.1, and initial work on Task 2.2 and Task 2.4, as described in the project proposal. The activities related to Task 1.1 are construction of a representative volume element (RVE) containing disordered fiber distributions, simulating manufacturing effects, and its computational micromechanics failure analysis. Task 2.2 is concerned with RVE level modeling by peridynamics and Task 2.4 addresses fatigue damage with peridynamics. Initial results for all tasks are reported and the ongoing work is outlined.					
<b>15. SUBJECT TERMS</b> Computational micromechanics, Cavitation induced cracking, Peridynamics, Fatigue cracking, Porous media.					
<b>16. SECURITY CLASSIFICATION OF:</b>			<b>17. LIMITATION OF ABSTRACT</b>	<b>18. NUMBER OF PAGES</b>	<b>19a. NAME OF RESPONSIBLE PERSON</b>
<b>a. REPORT</b>	<b>b. ABSTRACT</b>	<b>c. THIS PAGE</b>			William Nickerson
U	U	U	SAR	8	<b>19b. TELEPHONE NUMBER (Include area code)</b> 703-696-8485

**Quarterly Progress Report, April 1 – June 30, 2016**

**A Hybrid Approach to Composite Damage and Failure Analysis  
Combining Synergistic Damage Mechanics and Peridynamics**

Award Number N00014-16-1-2173

DOD – NAVY – Office of Naval Research

PI: Ramesh Talreja  
Co-PI: Florin Bobaru

Executive Summary

*The work performed in the reporting period has been focused on continuation of Task 1.1, and initial work on Task 2.2 and Task 2.4, as described in the project proposal. The activities related to Task 1.1 are construction of a representative volume element (RVE) containing disordered fiber distributions, simulating manufacturing effects, and its computational micromechanics failure analysis. Task 2.2 is concerned with RVE level modeling by peridynamics and Task 2.4 addresses fatigue damage with peridynamics. Initial results for all tasks are reported and the ongoing work is outlined.*

## **Task 1.1 Micro-level crack Initiation**

### **Background and motivation**

Manufacturing of polymer matrix composites (PMCs) results in disordered fiber distributions and defects such as voids in the matrix. We focus in this task on the local stress states in the matrix that become triaxial under any remotely applied stresses resulting from the service environment in which a given composite structure operates. The local stress states are responsible for the precursor mechanisms that initiate cracks. This task studies the point-failure processes that become critical under favorable energy conditions. The two basic energy-driven processes are cavitation and shear-band formation in polymers. The former is governed by the dilatation energy density, while the latter requires energy of distortion for its initiation.

The work conducted in the reporting period has focused on cavitation resulting in regions of fiber clusters, where favorable conditions for cavitation are likely. The remote loading considered in this work is tension normal to fibers (so-called transverse tension).

### **Approach and Results**

The approach taken here is to consider the type of fiber clusters that are likely to result from the manufacturing process. In most cases, the resin flow displaces fibers that are initially relatively ordered and are in contact with one another. The displacement caused by the resin flow induced forces will be the outward radial movement and the in-plane rotation of fibers. Both these displacement variables will be random, as the manufacturing process cannot be controlled in a deterministic way. In the simulation, a pre-specified range in both variables is implemented by using uniform random distributions.

Fig. 1 (a) below shows an initial (dry) cross-section of a circular region of a fiber bundle, and Fig. 1 (b) displays the disordered fiber distribution after the random displacements have been enforced. As can be seen, the post-manufacturing fiber distribution has clustered and diffused sub-regions. As reported in the 1<sup>st</sup> Quarterly Progress Report, the constraint caused by closeness of the fibers results in favorable conditions for cavitation.

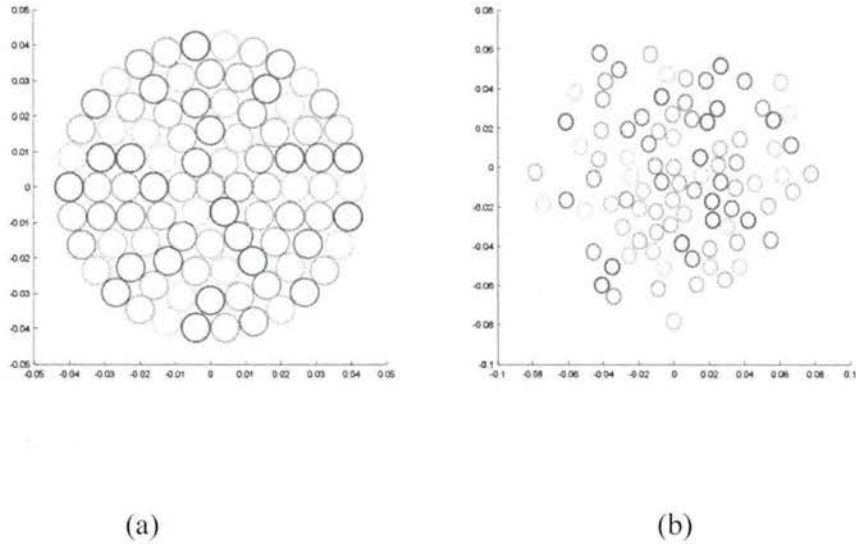


Fig. 1. (a) Initial region of a dry fiber bundle where all fibers are in contact, and (b) Simulated region of disordered fiber distribution using random outward radial movement and in-plane rotation of fibers.

Several realizations, such as that shown in Fig. 1 (b), were generated. The number of fibers used in each case was 91. Each RVE realization was analyzed with a finite element model, where the local stress states in the matrix were calculated and were utilized in the failure analysis.

The failure analysis consisted of determining which of the two mechanisms (cavitation and shear-banding) are likely to initiate first. Figure 2 shows the dilatational and distortional energy density variations with the remote tensile strain. The zero strain corresponds to thermal cooldown.

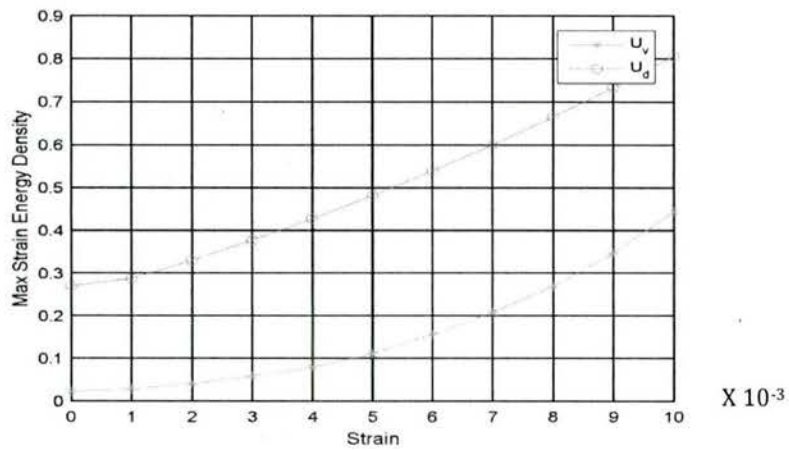


Figure 2. The variations with applied strain of the dilatational energy density (lower curve) and of the distortional energy density (upper curve). The criticality is reached at approximately 0.7% strain when the dilatational energy density reaches the experimentally determined critical value (0.2 MPa).

To validate whether the critical dilatational energy density represents hydrostatic tension, the three principal stresses are calculated and their pair-wise ratios are plotted in Fig. 3.

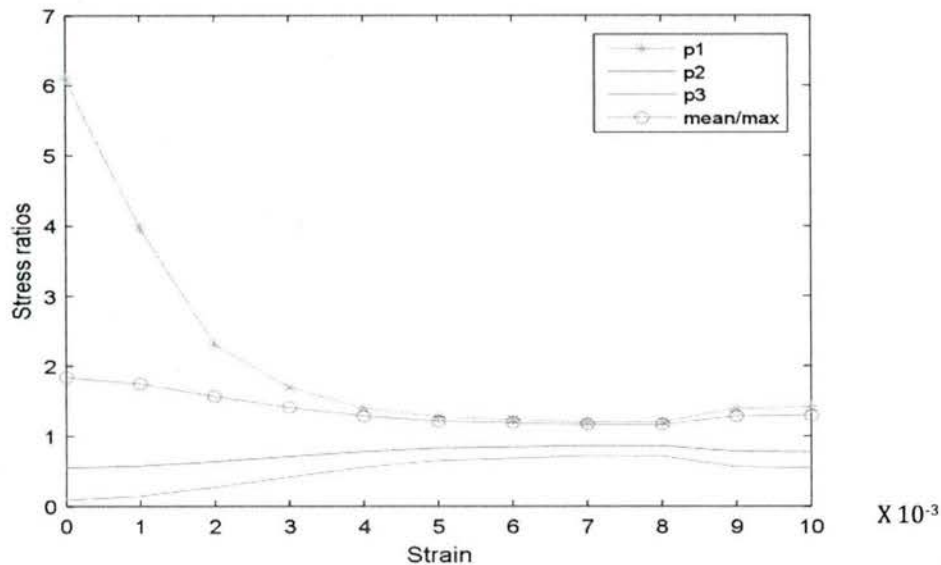


Figure 3. The pair-wise ratios of principal stresses and the ratio of the mean to max principal stress corresponding to the results in Fig. 2 are plotted. At 0.7% strain the triaxial stress state is not near enough to a hydrostatic state to favor cavitation.

The results shown in Fig.2 and Fig. 3 are for one realization of the RVE simulating a manufacturing induced disorder in fiber distribution. This realization illustrates unfavorable conditions for cavitation. A total of six realizations were performed. Two of the six did fall in a favorable region of cavitation.

The effect of cooldown temperature from processing to room temperature was also studied. The results above are for 82<sup>o</sup>C cooldown temperature, which is typical for glass-epoxy composites. However, this temperature can be varied. Today, resins are available to do room temperature curing of thermosetting resins. Therefore, the cooldown temperature was varied to see its effect on initiation of cavitation (and consequently, fiber-matrix debonding). Following summarizes the computed results.

When the cooldown temperature was reduced to 75<sup>o</sup>C, the favorable conditions for cavitation were found to occur earlier, at 0.6% strain. Further reducing the cooldown temperature, however, did not favor cavitation. On the other hand, increasing the cooldown temperature required increasing the mechanical load for cavitation to initiate. These results have important implications on the effect of manufacturing on failure initiation under transverse loading.

## **Ongoing work**

The effect of manufacturing defects on crack initiation will continue a little into the third quarter. Then, the focus will be on transverse crack formation and its multiplication in the presence of manufacturing defects.

**Task 2.2 RVE level modeling with peridynamics, and Task 2.4: Fatigue damage modeling with peridynamics.**

## **Motivation**

Pores, manufacturing defects, holes and round notches are locations where fatigue cracks may initiate from or arrest, depending on the loading conditions. Investigating the evolution of fatigue cracks after sinking into a hole, for example, is critical for predicting damage evolution in composite materials, in which pores, inhomogeneities and manufacturing defects play critical roles.

## **Approach and Results**

We have introduced a fatigue crack growth model based on peridynamics and validated our implementation against experimental results in terms of the crack path shape. We perform convergence studies in terms of the nonlocal region size for a modified compact tension test, which leads to curved fatigue crack paths. The experimental crack paths are strongly influenced by the location of a hole in the specimen, and the peridynamic results capture this sensitivity well (see Figure 4). Fatigue lifetimes obtained by the peridynamic model are in good agreement with experiments for different crack growth rates in different cycle ranges. Different from methods based on classical continuum mechanics, the peridynamic fatigue crack model does not require additional criteria to guide crack or damage growth. In particular, we use the peridynamic fatigue model, without any modifications, to simulate fatigue crack growth in a two-phase composite in which several crack initiation points exist and where fatigue crack paths interact in complex ways. We have published these results in reference [1].



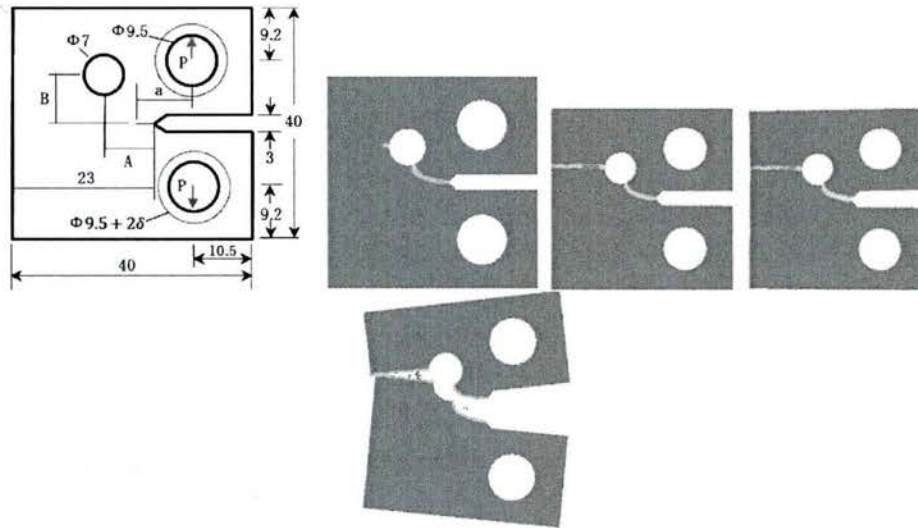


Fig. 5. Crack nucleation after the original crack sinks into the added hole. Damage index map showing the transition between fatigue crack growth and quasi-static fracture/final sample failure. Results to appear in [2].

Applied to a fiber-reinforced polymer composite material, the fatigue crack model produces results consistent with those seen in experiments (see Figs. 6 and 7). In Fig. 6, we show a sample RVE in which the red colored disks are the fiber cross-sections and the blue is the polymer matrix material.

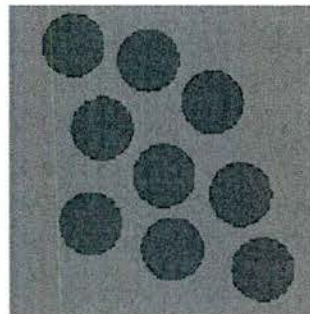


Fig. 6. Cross-section of an RVE in an FRC. Fatigue loadings are applied in the vertical direction.

The results in Fig. 7 show that fatigue cracks can initiate at multiple sites. The local arrangement of fibers leads to stress concentrations that produce matrix micro-cracks that join together in generating matrix macrocracks. Our peridynamic model captures this very well. It is interesting to also observe that, in certain cases, cracks grow around the fibers, indicative of fiber-matrix debonding failure. In the simulations shown in Fig. 7, the interface is slightly “stronger” than the matrix, and because of that, debonding is less dominant here. Our further studies will focus on the interface fatigue properties.

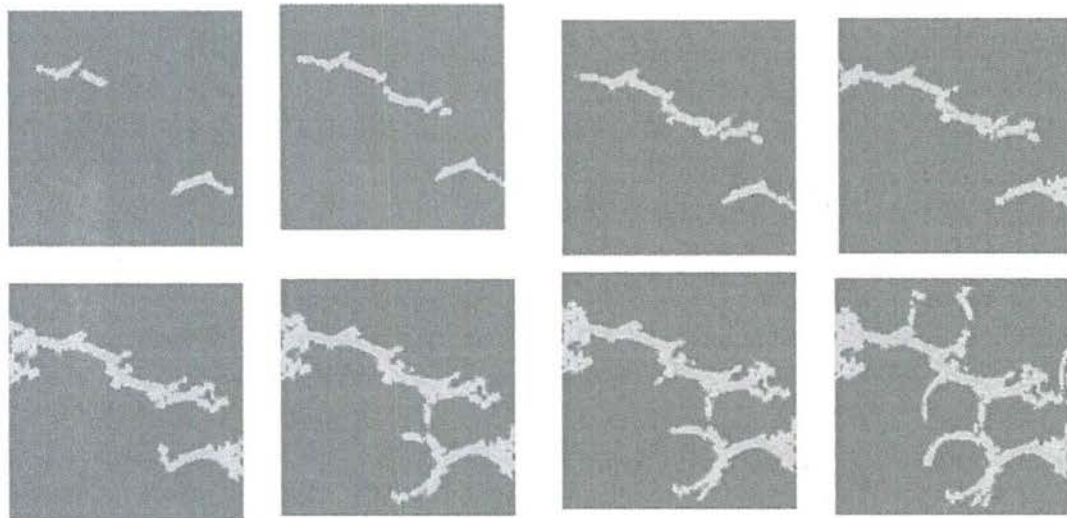


Fig. 7. Damage maps at different fatigue cycles showing fatigue crack nucleation at multiple sites, growth and coalescence of cracks. Fiber-matrix debonding is also observed.

### **Publications**

- [1] Zhang, G., Le, Q.V., Loghin, A., Subramaniyan, A., and Bobaru, F., "Validation of a peridynamic model for fatigue cracking", *Engineering Fracture Mechanics*, **162**: 76–94 (2016).
- [2] Zhang, G., and Bobaru, F., "Modeling the evolution of fatigue failure with peridynamics" *Romanian Journal of Technical Sciences - Applied Mechanics*.